IRANIAN JOURNAL OF CATALYSIS

Application of $Fe_3O_4/SiO_2/CeO_2$ nanocomposite, an efficient and magnetic catalyst, to synthesize 2,3-dihydroquinazolin-4(1*H*)-ones derivatives

Elham Mohamadzadeh, Zinat Gordi[*]

Department of Chemistry, Payame Noor University, PO Box 19395-3697, Tehran, Iran

ABSTRACT

A supported magnetic nanocomposite as a simple, stable, and efficient catalyst was successfully developed for condensation reaction of aldehydes, ammonium acetate, and isatoic anhydride to prepare 2,3-dihydroquinazolin-4(1*H*)-one derivatives as essential biologically active heterocyclic compounds. Ethanol as a non-toxic solvent under a reflux condition was utilized in the reactions. The $Fe_3O_4/SiO_2/CeO_2$ nanocomposite was prepared as a magnetic and novel catalyst. The value of components of the catalyst composite, including Fe_3O_4, SiO_2, and CeO_2, was optimized using experimental design to prepare the best catalyst composite with the highest reaction efficiency. The optimum amounts of Fe_3O_4, SiO_2, and CeO_2 in the catalyst composite were 0.37 g, 0.85 mL, and 1.28 g, respectively. The catalyst structure was characterized by FT-IR spectroscopy, vibrating sample magnetometer, Powder X-ray diffraction, and Transmission electron microscope. A sol-gel procedure was utilized to prepare the catalyst, in which chemical bonds between the catalysis components, leading to a high chemical, mechanical, and thermal stability of the catalyst. Several syntheses of 2,3-dihydroquinazolin-4(1*H*)-ones derivatives were performed using $Fe_3O_4/SiO_2/CeO_2$ (0.1 g) in EtOH (10.0 mL) under reflux for 9-19 min with yield in the range of 89-97%. The method displayed various advantages, including high yields, easy workup, low catalyst consumption, high catalyst reusability, low reaction times, and fast and straightforward catalyst separation using a magnet.

Keywords: Quinazolin-4(3H)-ones; 2,3-dihydroquinazolin-4(1H)-ones; Nanocomposite; Magnetic catalyst; $Fe_3O_4/SiO_2/CeO_2$; Aldehydes.

1. Introduction

Nanoparticulate supports were utilized in catalyst composites as an efficient bridge between homogeneous and heterogeneous catalysis [1]. In conventional procedures, the nanocatalyst supported is usually separated from products after the reaction completion by filtration and centrifugation methods, which are difficult, expensive, and time-consuming. [2]. The use of magnetic nanoparticles (MNPs) as a nanocatalyst or nanocatalyst core leads to easy and rapid separation of the catalyst after completing the reaction by a proper magnet [3]. This procedure can eliminate the drawbacks of conventional catalysts. Magnetic nanoparticles are highly favorable materials to attach homogeneous inorganic and organic-containing catalysts [4].

Therefore, the MNPs separation with an external magnetic field is a simple, economical, fast, and suitable procedure with a proper separation for industrial applications. Besides, the strategy is more impressive and accessible than centrifugation or filtration techniques for catalyst separation [5-7].

Superparamagnetic iron oxide showed acceptable properties as magnetic nanoparticle support in the catalyst composites with high performance [8]. Fe_3O_4 NP as catalyst support has high advantages such as low cost, simple preparation, low toxicity, high surface area, and suitable stability with an appropriate magnetic property for the straightforward separation of catalyst without filtration or centrifugation methods [9]. These features of Fe_3O_4 NPs have led to much attention to it as an ideal support to heterogenize homogeneous catalysts [10]. The chemical co-precipitation strategy to prepare Fe_3O_4 NPs is a straightforward and efficient procedure [11]. However, Fe_3O_4 NPs were aggregated in the

[*]Corresponding author:
E-mail address: *Gordi_z@yahoo.com* (**Z. Gordi**)

solution due to the high surface area and superparamagnetism properties [12, 13]. Magnetic Fe_3O_4 NP aggregation is a critical disadvantage that reduces the catalyst ability and reaction efficiency due to decreasing the surface area between the catalyst and the reactants. The instability of this support is another limitation to applying Fe_3O_4 NP that reduces the catalyst reusability [12]. Therefore, coating the magnetic Fe_3O_4 NP surface as catalyst support with suitable compounds such as inorganic or inorganic shells to prepare a catalyst is a proper strategy to prevent the magnetic Fe_3O_4 NP agglomeration and increase its stability [14]. Besides, the superparamagnetism properties of Fe_3O_4 NP in the catalyst composite leads to a high catalyst recovery to recycle and reuse, employing a strong magnet [15].

Performing organic reactions for synthesizing target organic materials in aqueous media is a proper strategy with various advantages because water as a solvent is abundant, cheap, economical, safe, non-toxic, environmentally friendly solvent. Due to the high polarity, appropriated boiling point, suitable density, hydrogen bond formation with other reagents, water as a green solvent also presents unique selectivity and reactivity compared to other conventional solvents [16]. Thus, the development of a new catalyst with high stability in water samples, low cost, and simple recyclability is of great interest to enhance the reaction efficiency.

2,3-Dihydroquinazolinones as a critical group of materials with various bioactivities were utilized to treat human cancer and regulate plant growth [17]. Besides, they are easily converted to quinazolin-4(3H)-one analogues by the oxidation process [18]. Quinazolin-4(3H)-one analogues are present in various natural products and display biological activity [19, 20]. Remarkably, the scaffold of quinazolinone core was used in medicinal chemistry as a drug-like template [21]. Various catalysts, including Brønsted acid [22], $CoAl_2O_4$ nanoparticles[23], acidic ionic liquid [24], Fe_3O_4 NPs [25], montmorillonite-K10[26], silica sulfuric acid [27], and aluminum tris(dihydrogen phosphate) [28], were reported for the 2,3-Dihydroquinazolinones synthesis in the one-pot reaction. The most disadvantages of the methods are that some of these methodologies involve strongly acidic conditions, toxic catalysts, hazardous organic solvents, and long reaction times. Some disadvantages of the methods are high reaction time, use of toxic and unstable catalysts, consumption of hazardous and expensive solvents and reaction in difficult conditions, especially acidic media. Therefore, the synthesis of new

catalysts with suitable properties can be regarded to overcome some of the limitations of these methods.

Here, we reported the $Fe_3O_4/SiO_2/CeO_2$ nanocomposite as a stable and efficient catalyst for synthesizing 2,3-dihydroquinazolin-4(1H)-one derivatives. A sol-gel and chemical procedure was applied to synthesize the catalyst based on a chemical bonding formation between catalyst components, enhancing the catalyst stability. Due to the high chemical, mechanical, and thermal stability of the prepared catalyst, it can be reused without significant degradation and inactivity several times and also minimizes environmental damages. The magnetic catalyst is readily and straightforwardly separated from the media using a simple magnetic decantation procedure, reducing the separation time and increasing the separation efficiency by eliminating the centrifuge or filtration step (**Scheme 1**). The catalyst composite was optimized using an optimal mixture design to prepare the best catalyst with high reaction efficiency, fast and straightforward separation, and increased stability. The catalyst showed a high yield under low reaction time in non-toxic solvent and mild conditions. Besides, the catalyst was synthesized by a straightforward method with low reagent consumption and price.

2.Experimental

2.1.Materials and instruments

The employed high purity commercial reagent grade chemicals were purchased from Merck and Fluka. Millipore water (18.2 MΩ cm) was used throughout the experiment. ^{1}HNMR spectra were recorded with a Bruker DRX-400 spectrometer. FT-IR spectra were obtained with potassium bromide pellets in the range of 400–4000 cm-1 with a Perkin-Elmer 550 spectrometer. Nanostructures were characterized by Fourier transform infrared spectroscopy (FT-IR), TEM – model -912AB /LEO, X-ray powder diffraction (XRD), and vibrating sample magnetometer (VSM).

2.2.Preparation of Fe₃O₄ nanoparticles

A chemical co-precipitation strategy as a straightforward method was applied to prepare the magnetic Fe_3O_4 nanoparticles as the catalyst support. For this purpose, $FeCl_2$ (2.0 g) and $FeCl_3$ (5.2 g) were thoroughly dissolved into distilled water (25.0 mL) containing concentrated HCl (0.85 mL, 12.1 M). Sodium hydroxide solution (25.0 mL, 1.5 M) was added dropwise into the resulting solution under stirring at room temperature. The mixture was transferred into a water bath for 30 min at 70 ºC. The magnetic Fe_3O_4 NPs were separated from the solution by a magnet and rinsed

Scheme 1 Synthesis of 2,3-dihydroquinazolin-4(1*H*)-ones

three times with deionized water, followed by HCl solution (4 wt%) 5 times. The magnetic Fe_3O_4 NPs were then washed with deionized water several times to neutralize the pH of the solution. Finally, the magnetic Fe_3O_4 NPs (loose brown powder) was dried in an oven at 70 ºC [29].

2.3. Preparation of $Fe_3O_4/SiO_2/CeO_2$ composites

Fe_3O_4/SiO_2 nanocomposites were prepared through a sol-gel method according to the previous research [30]. Briefly, the magnetic Fe_3O_4 NPs (0.37 g) were ultrasonically dispersed into a solution containing ethanol (50.0 mL), distilled water (9.0 mL), and concentrated ammonium hydroxide solution (1.0 mL, 28 wt%) for 30 min, followed by the addition of tetraethyl orthosilicate (0.85 mL) under stirring at 400 rpm at room temperature for 24 h. The precipitate (Fe_3O_4/SiO_2 nanocomposite) was separated by a magnet and washed twice with ethanol and distilled water before drying for 12 h at 70 ° C. To prepare the $Fe_3O_4/SiO_2/CeO_2$ NPs, 1.0 g of the Fe_3O_4/SiO_2 nanocomposite were poured in deionized water (100 mL) and sonicated for 30 min at room temperature. Then, 1.28 g of Cerium (III) nitrate hexahydrate was added into the suspension, followed by stirring at 70 ºC for 1 h under N_2. Concentrated ammonium hydroxide solution (5.0 mL, 28 wt%) was slowly added into the mixture and stirred at 300 rpm for 3 h at 70 ºC. The precipitate was separated and rinsed three times with distilled water and dried in an oven under vacuum at 70 ºC for 8 h. The obtained precipitate was finally calcinated at 450 ºC under N_2 gas flow for 2 h to prepare $Fe_3O_4/SiO_2/CeO_2$ nanocomposite[31].

2.4. Optimization of the catalyst composite

The catalyst plays a critical role in reaction efficiency. Therefore, the type of components and their percentages in the catalyst composite is crucial in successfully performing a high-efficiency reaction. An experimental design strategy based on an optimal mixture design was generated to optimize the amount of each component,

including Fe_3O_4 nanoparticles, TEOS, and CeO_2 in the catalyst. The amount of each component and the design are shown in **Table 1**. The amount of each component and the reaction efficiency were selected as independent and dependent factors, respectively. Each run in **Table 1** indicated the amount of each component in the catalyst and was used in the reaction between isatoic anhydride, 4-chlorobenzaldehyde, and ammonium acetate according to section 2.5. Other reaction conditions such as reaction time, solvent, and catalyst amount were constant in 16 min, H_2O, 0.1 g under reflux, respectively. Analysis of variance was utilized to evaluate the results at the 95 % confidence interval. The obtained results of ANOVA are presented in **Table 2.** The p-value is an essential parameter in the Table to determine the significant effects of each component or binary interactions[32-34]. A factor or interaction with the p-value less than α-level (0.05) at the 95 % confidence limit significantly affects the reaction efficiency. Therefore, the presented model, linear mixture of components, and all binary interactions have significant effects on the reaction efficiency. In other words, all three components of the catalyst affect the extraction efficiency, and the removal of each component in the prepared catalyst can lead to a reduction in the reaction efficiency. The effects of changes in the value of each component on the reaction efficiency are shown by a quadratic equation as follows:

RE= -30.1386 * Fe_3O_4 -0.14278 * TEOS + 28.6175 * CeO_2 + 153.177 * Fe_3O_4 * TEOS + 248.516 * Fe_3O_4 * CeO_2 + 247.372 * TEOS * CeO_2 **Eq. 1**

This equation fits in well with the results because its R^2 and adjusted R^2 values are 0.9787 and 0.9680, respectively. This equation shows that the amount of CeO_2 has the most significant impact on the reaction efficiency because its coefficient (+26.6175) is the highest in the reaction equation. Also, CeO_2 in the catalyst composite has a considerable effect on increasing the efficiency of the reaction. The simultaneous effects of all three components on the reaction efficiency are shown in the three-dimensional

Table 1. The selected level of each component in the catalyst nanocomposite and optimal mixture design

Component	Name	Units	Minimum	Maximum
A	Fe_3O_4	g	0.3	0.8
B	TEOS	mL	0.7	1.2
C	CeO_2	g	1	1.5
			Total	2.50

Experimental Run	Fe_3O_4	TEOS	CeO_2	RE%[1]
1	0.8	0.7	1	75
2	0.3	0.7	1.5	78
3	0.55	0.95	1	77
4	0.3	0.95	1.25	80
5	0.8	0.7	1	75
6	0.55	0.7	1.25	79
7	0.55	0.7	1.25	79
8	0.55	0.95	1	77
9	0.3	0.95	1.25	79
10	0.63	0.78	1.09	78
11	0.3	1.2	1	76
12	0.55	0.7	1.25	79
13	0.47	0.86	1.17	79
14	0.42	1.08	1	77
15	0.38	0.78	1.34	80
16	0.3	1.1	1.1	78

[1] Reaction efficiency

Table 2. Analysis of variance for evaluating results

Source	Sum of Squares	df	Mean Square	F-value	p-value	Significant
Model	36.95	5	7.39	91.88	< 0.0001	+
Linear Mixture	22.15	2	11.07	137.69	< 0.0001	+
AB	3.35	1	3.35	41.66	< 0.0001	+
AC	9.49	1	9.49	118.05	< 0.0001	+
BC	7.26	1	7.26	90.28	< 0.0001	+
Residual	0.8042	10	0.0804			
Lack of Fit	0.3042	5	0.0608	0.6085	0.7005	-
Pure Error	0.5000	5	0.1000			
Cor Total	37.75	15				

graph (**Fig. 1**). According to **Fig.1** and Eq. 1, the optimum amount of each component, including Fe_3O_4, TEOS, and CeO_2, in the catalyst composite was determined to be 0.37 g, 0.85 mL, and 1.28 g, respectively. The optimum amounts were used in section 2.3 to prepare the $Fe_3O_4/SiO_2/CeO_2$ composites.

Selected spectral data

2-(2-Hydroxyphenyl)-2,3-dihydroquinazolin-4(1H)-one (No. 9):

IR (KBr) cm^{-1}: 3500, 3279, 3065, 1639, 1422. ^{1}H NMR (400 MHz, DMSO-d_6): δH = 6.12 (s, 1 H), 6.62 (t, J = 7.5 Hz, 1H), 6.81 (m, 3H), 6.89 (d, J = 8 Hz, 1H), 7.17 (m, 2H), 7.41 (d, J = 7.5 Hz, 1H), 7.70 (d, J = 7.5 Hz, 1 H), 8.01 (s, 1H), 9.77 (s, 1H) ppm.

2-(4-methylphenyl)-2,3-dihydroquinazolin-4(1H)-one (No. 6):

IR (KBr) cm^{-1}: 3313, 1658, 1611, 1439. ^{1}H NMR (400 MHz, DMSO-d_6): δH = 8.21 (s, 1H), 7.62-7.59 (d, J = 7.5, 1H), 7.38-7.35 (d, J = 7.5, 2H), 7.26-7.14 (m, 3H), 7.03 (s, 1H), 6.75-6.64 (m, 2H), 5.71 (s, 1H), 2.49-2.42 (s, 3H) ppm.

2-(4-bromophenyl)-2,3-dihydoquinazolin-4(1H)-one (No. 10):

IR (KBr) cm^{-1}: 3310, 1656, 1608, 1433. ^{1}H NMR (400 MHz, DMSO-d_6): δH= 8.17-8.14 (m, 1H), 7.80-7.78 (m, 1H), 7.63-7.59 (m, 3H), 7.47-7.44 (m, 2H), 7.30-7.24 (m, 1H), 6.77-6.72 (d, J = 18.9, 1H), 6.71-6.68 (m, 1H), 5.76 (s, 1H) ppm.

2-(4-chlorophenyl)-2,3-dihydoquinazolin-4(1H)-one (No. 11):

IR (KBr) cm^{-1}: 3309, 1655, 1611, 1435. ^{1}H NMR (400 MHz, DMSO-d_6): δH = 8.29 (s, 1H), 7.61-7.43 (m, 5H), 7.26-7.20 (t, J = 7.5, 1H), 7.12 (s, 1H), 6.75-6.63 (m, 2H), 5.75 (s, 1H) ppm.

2-(2,4-dichlorophenyl)-2,3-dihydroquinazolin-4(1H)-one (No. 14):

IR (KBr) cm^{-1}: 3341, 3180, 3059, 1663, 1429. ^{1}H NMR (400 MHz, DMSO-d_6): δH = 6.3 (s, 1H), 6.71–6.80 (m, 2H), 7.08 (s, 1 H, NH), 7.22–7.27 (t, J = 7.5 Hz, 1 H), 7.45-7.48 (dd, J1 = 8 Hz, J1 = 2 Hz, 1H), 7.66-7.69 (m, 3 H), 8.29 (s, 1 H) ppm.

3. Results and Discussion

3.1.The $Fe_3O_4/SiO_2/TiO_2$ nanocomposite characterization

The as-prepared $Fe_3O_4/SiO_2/TiO_2$ nanocomposite particles were characterized to evaluate the success of synthesis, chemical structure, and morphology by various techniques. **Fig. 2** presents the XRD patterns at several steps of the catalyst preparation of Fe_3O_4 NPs (a), $Fe_3O_4@SiO_2$ NPs (b), and $Fe_3O_4@SiO_2@CeO_2$ nanocomposites(c). The XRD pattern results indicated that the magnetite Fe_3O_4 NPs (JCPDS No. 72-2303) with the cubic spinel structure was prepared in the first step (**Fig. 2a**). The diffraction peaks of Fe_3O_4 NPs are presented with a 2θ of 18.3, 30.1, 35.4, 37.0, 43.0, 53.4, 56.9, 62.5, and 73.9, assigned to 111, 220, 311, 222, 400, 422, 511, 440 and 533 planes of Fe_3O_4 NPs, respectively[35]. The board peak with low intensity at 2θ value between 20 to 30 is related to SiO_2 with an amorphous structure [36]. Besides, a reduction in the peak intensity of Fe_3O_4 NPs was displayed due to coating these nanoparticles with SiO_2 in $Fe_3O_4@SiO_2$ NPs(**Fig. 2b**). Other diffraction peaks at 2θ of 28.6, 33.1, 47.6, 56.5, 59.3, and 69.6 correspond to CeO_2 NPs in the $Fe_3O_4@SiO_2@CeO_2$ pattern (**Fig. 2c**). The peaks of SiO_2 and Fe_3O_4 NPs are presented in **Fig. 2c**, while their intensities compared with **Fig. 2a** and **2b** were attenuated due to coating these nanoparticles with CeO_2.

Characterization of $Fe_3O_4/SiO_2/CeO_2$ nanocomposite was further evaluated using Transmission electron microscopy (TEM). In **Fig. 3(a)**, the SiO_2 layer was successfully encapsulated on the Fe_3O_4 core with a layer distance of about 14 nm, indicating the core and shell of Fe_3O_4/SiO_2 nanocomposite were Fe_3O_4 NPs and SiO_2, respectively. According to **Fig. 3(b)**, the CeO_2-coated Fe_3O_4/SiO_2 nanocomposite exhibited three parts with a core-shell magnetic structure, in which many small CeO_2 nanoparticles are the outer part of the prepared nanocomposite. Besides, CeO_2 NPs have a size of less than 10 nm, and some of them were aggregated together.

The magnetic properties of the catalyst were investigated by a vibrating sample magnetometer. **Fig. 4** presented the magnetic hysteresis loops of the catalyst components (Fe_3O_4 NPs and Fe_3O_4/SiO_2 nanocomposite) and the catalyst ($Fe_3O_4/SiO_2/CeO_2$ nanocomposite), which had saturation magnetizations (Ms) of 52.1290, 40.1530, and 8.9046 emu/g, respectively. A reduction in the Ms values of Fe_3O_4/SiO_2 nanocomposite and $Fe_3O_4/SiO_2/CeO_2$ nanocomposite were displayed in comparison with the Ms value of Fe_3O_4 NPs because the Fe_3O_4 NPs as the magnet core of catalyst was subsequently coated as a layer of SiO_2 and CeO_2 NPs in the Fe_3O_4/SiO_2 nanocomposite and $Fe_3O_4/SiO_2/CeO_2$ nanocomposite,
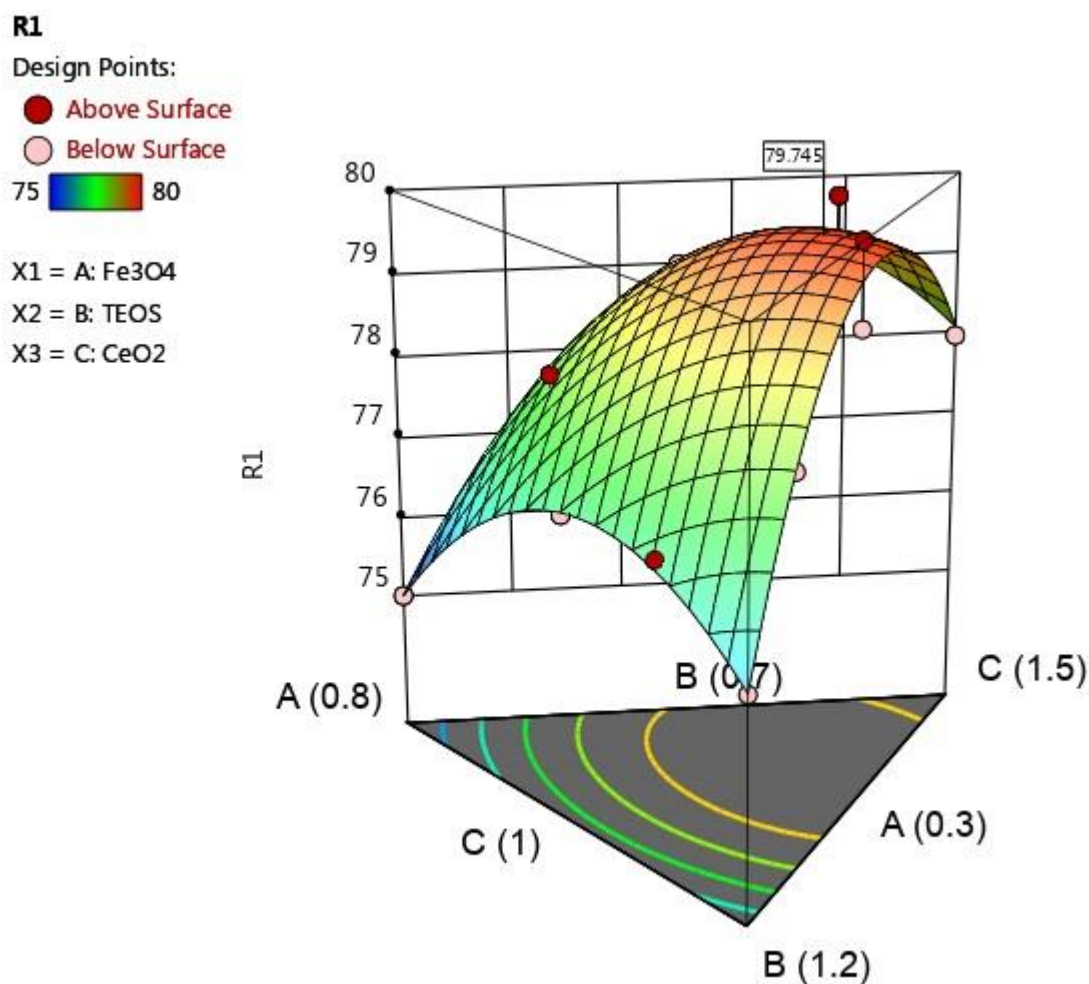
Fig. 1 The simultaneous effects of all catalyst components on the reaction efficiency
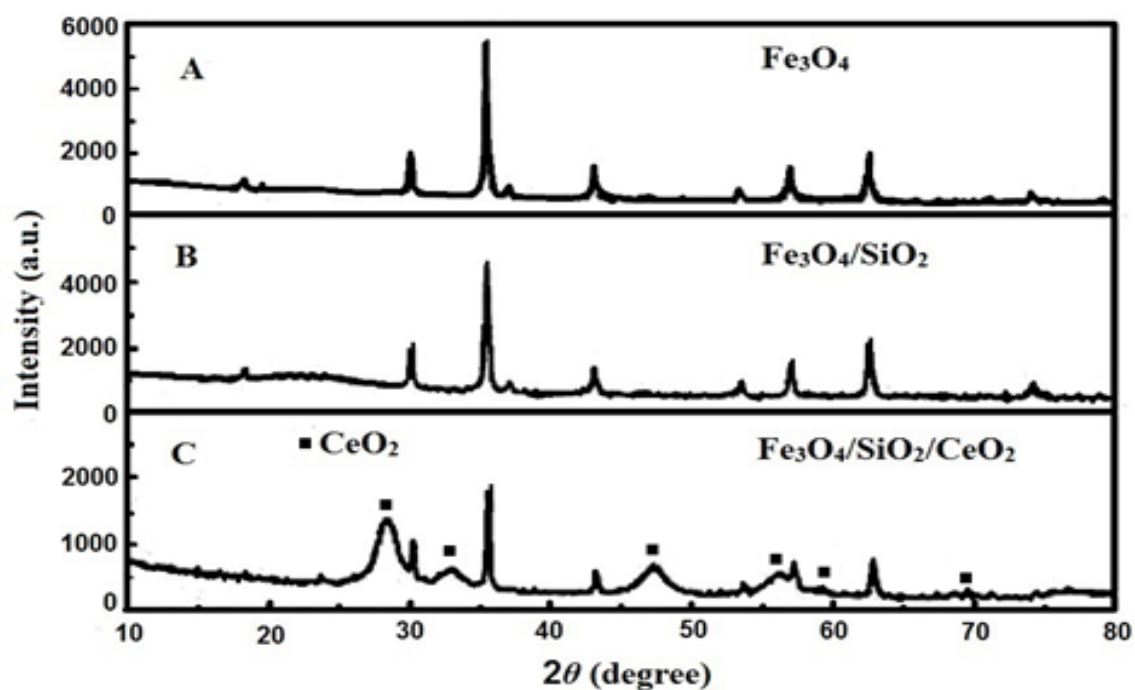
Fig. 2 XRD of (a) pure Fe_3O_4 NPs, (b) Fe_3O_4/SiO_2 nanocomposite, and (c) $Fe_3O_4/SiO_2/CeO_2$ nanocomposite
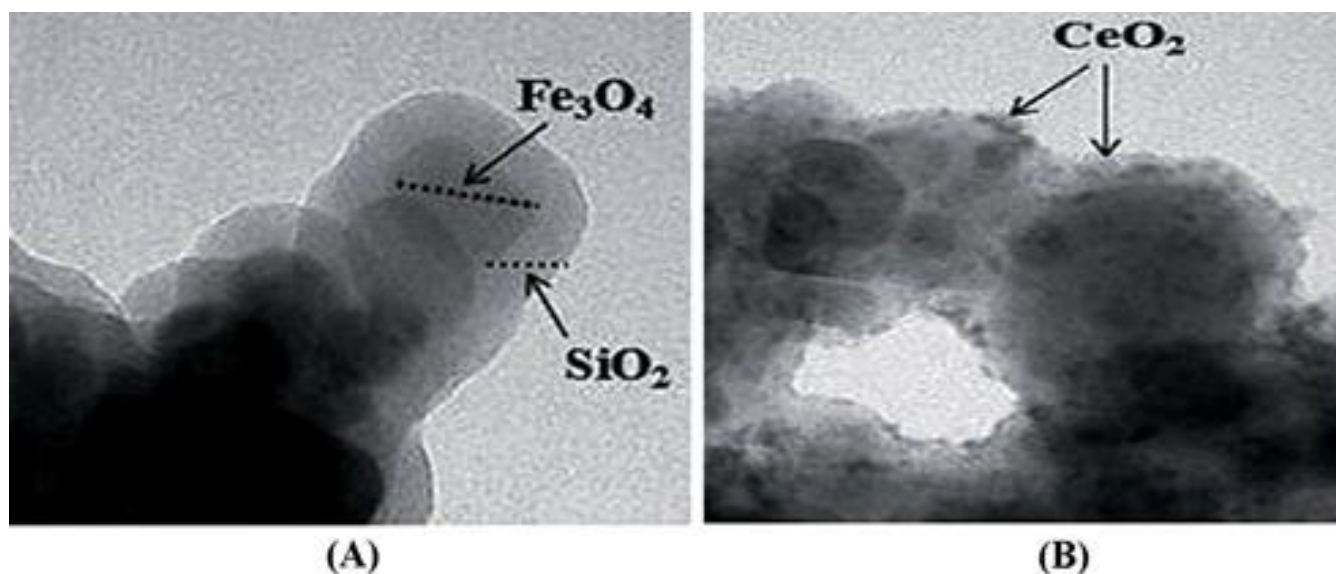
Fig. 3 TEM images of Fe_3O_4/SiO_2 nanocomposite (a) and $Fe_3O_4/SiO_2/CeO_2$ nanocomposite (b)
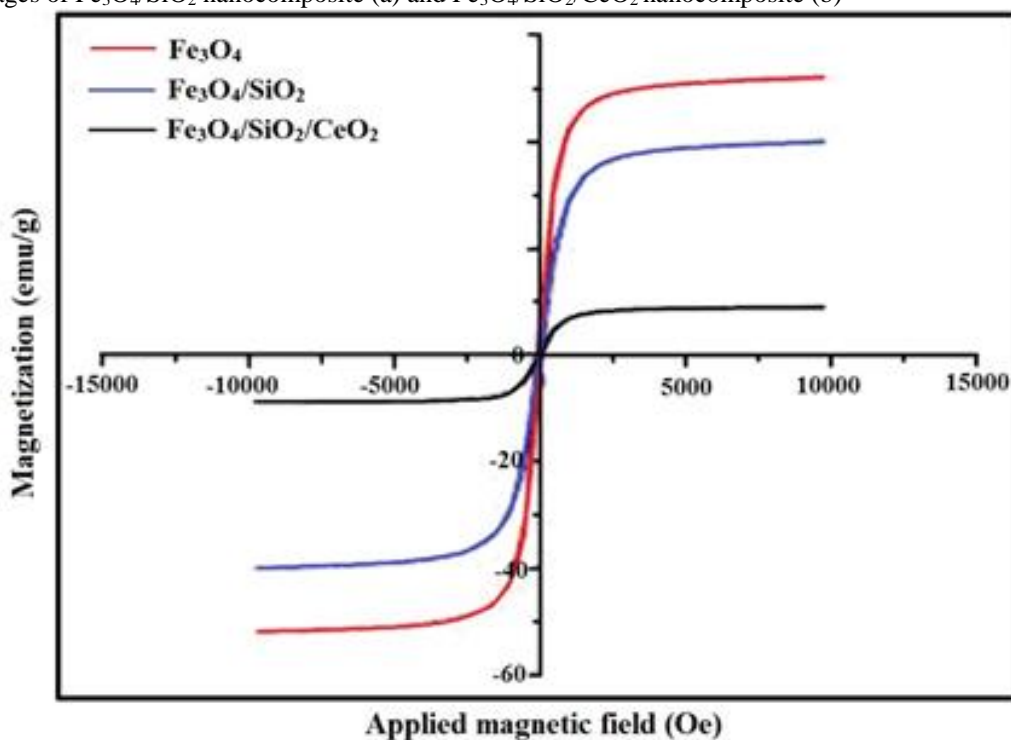
Fig. 4 Hysteresis loops of Fe_3O_4 NPs, Fe_3O_4/SiO_2 nanocomposite, and $Fe_3O_4/SiO_2/CeO_2$ nanocomposite.

which resulted in a reduction of their magnetism properties.

The FT-IR spectra of the catalyst components and the catalyst are presented in **Fig. 5.** Two adsorption bands at 1640 and 3428 Cm^{-1} are related to the stretching vibration of the hydroxyl group and bending vibration of H-O-H due to adsorbed or free water in Fe_3O_4 NPs, Fe_3O_4/SiO_2 nanocomposite, and the catalyst, respectively. The strong peaks at 590 Cm^{-1} in Fe_3O_4 NPs, Fe_3O_4/SiO_2 nanocomposite, and the catalyst are related to the Fe-O groups. An antisymmetric stretching vibration of the Si-O-Si group is shown at 1088 Cm^{-1} with a sharp band, confirming the SiO_2 existence in the Fe_3O_4/SiO_2 nanocomposite (**Fig. 5b**). The vibration band at 1475 Cm^{-1} corresponds to the stretching vibration of the Ce-O group in the $Fe_3O_4/SiO_2/CeO_2$ nanocomposite as the catalyst (**Fig. 5c**). Besides, the peaks at 1088 and 590 Cm^{-1} in **Fig.5 c** shifted to lower wavenumbers than **Fig. 5 b,** confirming the successful coating of the Fe_3O_4/SiO_2 nanocomposite with CeO_2.

3.2.Investigation of reaction conditions
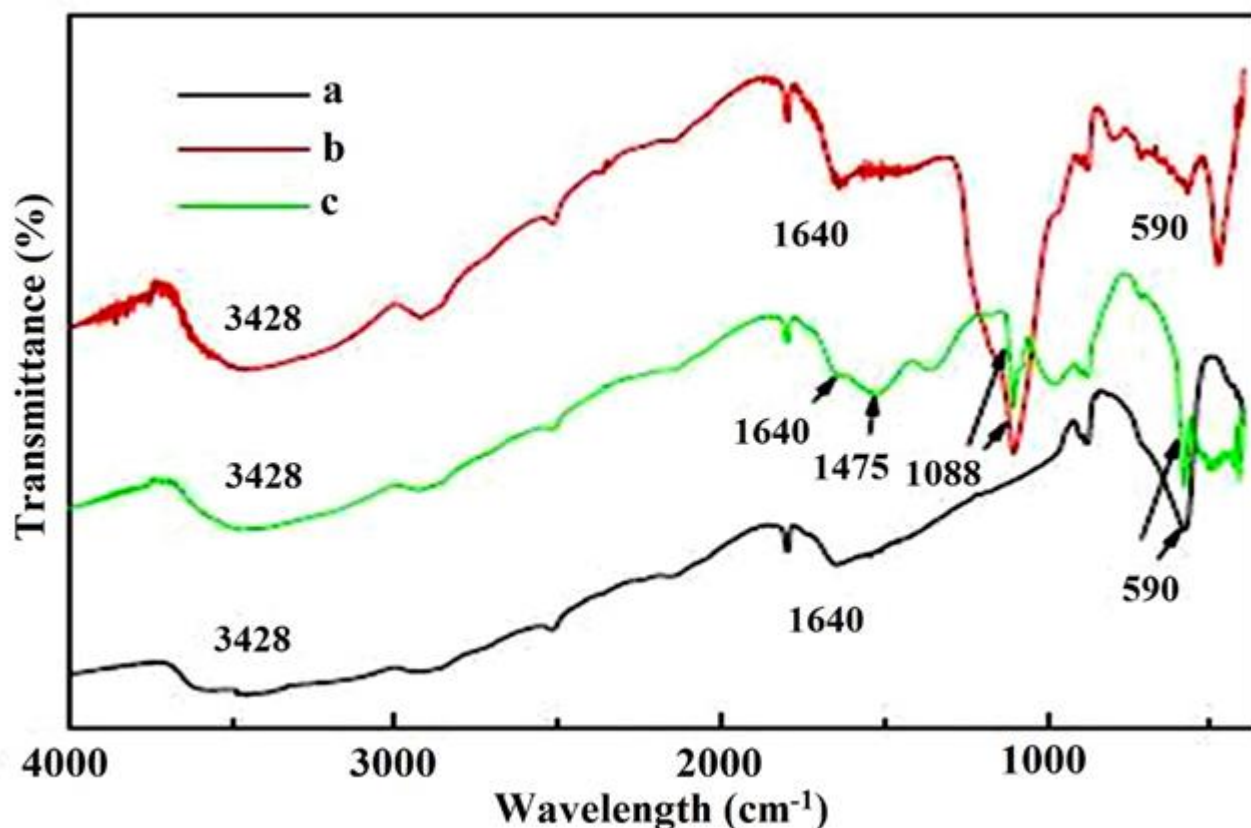
Fig. 5 FI-TR spectra of (a) Fe_3O_4 NPs, (b) Fe_3O_4/SiO_2 nanocomposite and (c) $Fe_3O_4/SiO_2/CeO_2$ nanocomposite

After the characterization of the nanocatalyst, different conditions, including the catalyst amount, temperature, and solvent type as independent factors for the model reaction of ammonium acetate, isatoic anhydride, and 4-chlorobenzaldehyde were evaluated to synthesize the product (No. 11) and optimize the reaction conditions by performing the reaction (**Table 3**). In the catalyst absence, the product yield was low under a reflux condition after 60 min (**Table 3**, entry 1), confirming that using the catalyst is essential to achieve high efficiency. The highest yield for the reaction was obtained when the reaction was under reflux conditions using 0.1 g of $Fe_3O_4/SiO_2/CeO_2$ nanocomposite (**Table 3**, entry 7). Then, several solvents such as EtOH, CH_3CN, H_2O, THF, and CH_2Cl_2 were used to investigate the solvent effects on the efficiency of the model reaction. In this study, ethanol is the best solvent with a yield of 95 % and a proper time of 12 min.

The catalyst reusability was studied based on catalyst separation after completion of the reaction and its reuse in the following reaction cycle. After separating the catalyst by a magnet, hot ethanol was used to resin the catalyst before drying at 80 ºC under vacuum for 2 h. Then, the catalyst was reused in the same reaction under optimization conditions (**Fig. 6**). The catalyst displayed

suitable stability for 5 cycles of reuse without a meaningful change in its activity.

3.3.Investigation of the reaction mechanism

The plausible mechanism for forming 2,3-dihydroquinazolin-4(1*H*)-ones is presented in **Scheme 2**. The $Fe_3O_4/SiO_2/CeO_2$ nanocomposite as the catalyst was activated the carbonyl group of isatoic anhydride through interact Ce (IV) or iron ion species as Lewis acid with non-bonding electron pairs of oxygen in carbonyl group to attack the ammonium acetate. Intermediate **I** was formed, followed by the decarboxylation to form 2-amino-*N*-substituted-benzamide (**II**). Similarly, Ce (IV) and iron ion species interacted with the carbonyl group in the aldehyde to active the aldehydes. The activated aldehyde was attacked to the amine group of Intermediate **II,** leading to the imine group in Intermediate **III,** which converted to product **4** [37-40]**.** The results in section 2.4 indicated that the CeO_2 amount in the catalyst nanocomposite has the highest and most significant effects on the reaction efficiency. According to the suggested mechanism, the catalytical activity of Ce (IV) ions as the Lewis acid is higher than iron ion species in Fe_3O_4 NPs or SiO_2 in the catalyst nanocomposite.

Table 3 Condensation of isatoic anhydride, 4-chlorobenzaldehyde, and ammonium acetate under various reaction conditions.

Entry	Catalyst (g)	Solvent	T (°C)	Time (min)	Yield[1]
1	None	EtOH	Reflux	60	13
2	0.06	EtOH	rt.	45	55
3	0.06	EtOH	50	35	61
4	0.06	EtOH	Reflux	27	75
5	0.10	EtOH	rt	30	70
6	0.10	EtOH	50	23	89
7	0.10	EtOH	Reflux	12	95
8	0.14	EtOH	rt	30	71
9	0.14	EtOH	50	25	90
10	0.14	EtOH	Reflux	15	95
11	0.10	H_2O	Reflux	16	80
12	0.10	CH_2Cl_2	Reflux	20	51
13	0.10	CH_3CN	Reflux	22	58
14	0.10	THF	Reflux	18	55

[1]   Isolated yields
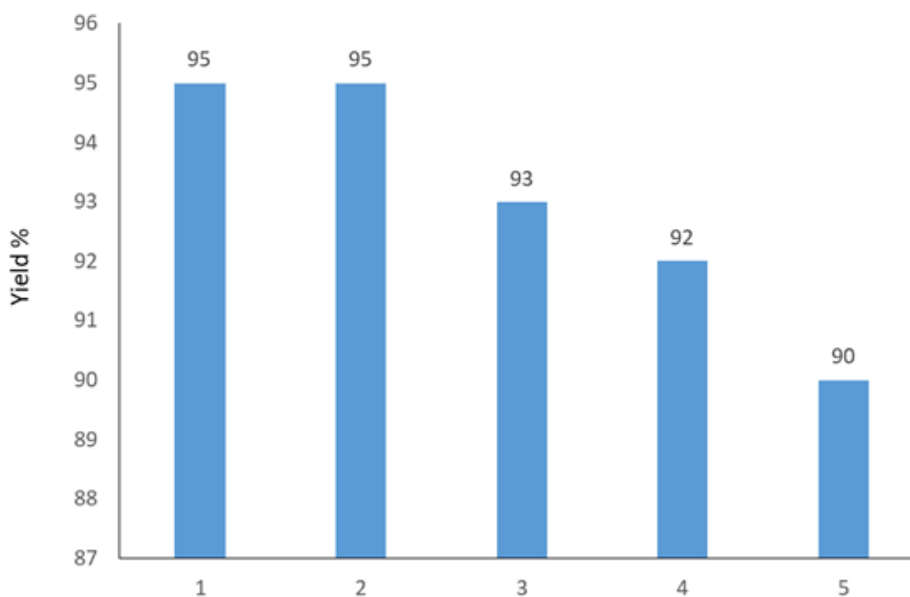
Fig. 6 The reusability of the catalyst in the synthesis of 2-(4-chlorophenyl)-2,3-dihydoquinazolin-4(1*H*)-one

3.4.Preparation of 2,3-dihydroquinazolin-4(1H)-one derivatives procedure

$Fe_3O_4/SiO_2/CeO_2$ (0.1g) as the catalyst was poured into a solution of isatoic anhydrides (5.5 mmol), aldehydes (5.0 mmol), and ammonium acetate (6.0 mmol) in 10.0 mL of ethanol as a green solvent, followed by refluxing for the specified period of time. The reaction conditions are presented in **Table 3**. The reaction progress was examined using TLC. The mixture was thoroughly cooled to ambient temperature before adding deionized water (10.0 mL) to it. The precipitate was carefully filtered and finally recrystallized in ethanol (**Scheme 1**).

Several syntheses of 2,3-dihydroquinazolin-4(1*H*)-ones derivatives from the condensation reaction of isatoic

anhydride with a wide range of aromatic aldehydes and ammonium acetate were examined utilizing $Fe_3O_4/SiO_2/CeO_2$ nanocomposite as the catalyst in EtOH under reflux conditions.

All reactions were completed in the range of 9-19 min, indicating that isatoic anhydride was efficiently reacted with various aromatic aldehydes containing withdrawing or electron-donating substituents to form cyclo condensation products at a low reaction time and high yields (**Table 4**). The methods' advantages included simple catalyst synthesis, low catalyst consumption, suitable catalyst reusability, and straight and fast separation of the catalyst with a magnet, making the method valuable for synthesizing 2,3-dihydroquinazolin-4(1*H*)-one derivatives.

4. Conclusions

We have found an efficient, inexpensive, and straightforward procedure for one-pot synthesis of 2,3-

dihydroquinazolin-4(1*H*)-ones using $Fe_3O_4/SiO_2/CeO_2$ nanocomposites as a catalyst. The catalyst composite was optimized with an experimental design based on optimal mixture design. The procedure can be utilized for a wide range of aromatic aldehydes and amines, and the products are obtained in high yields with a suitable reaction time. Besides, the catalyst was synthesized using a simple and straightforward procedure without the need for sophisticated devices. Using a chemical approach to prepare the catalyst, including co-precipitation, sol-gel, and chemical reaction, leads to the high stability of catalyst for reuse the catalyst for 5 times without a meaningful reduction in its activities. Moreover, a low amount of catalyst consumption, low reaction time, facile catalyst separation, and toxic solvent-free are other advantages of this procedure, confirming that the proposed method agrees with the principles of green chemistry.
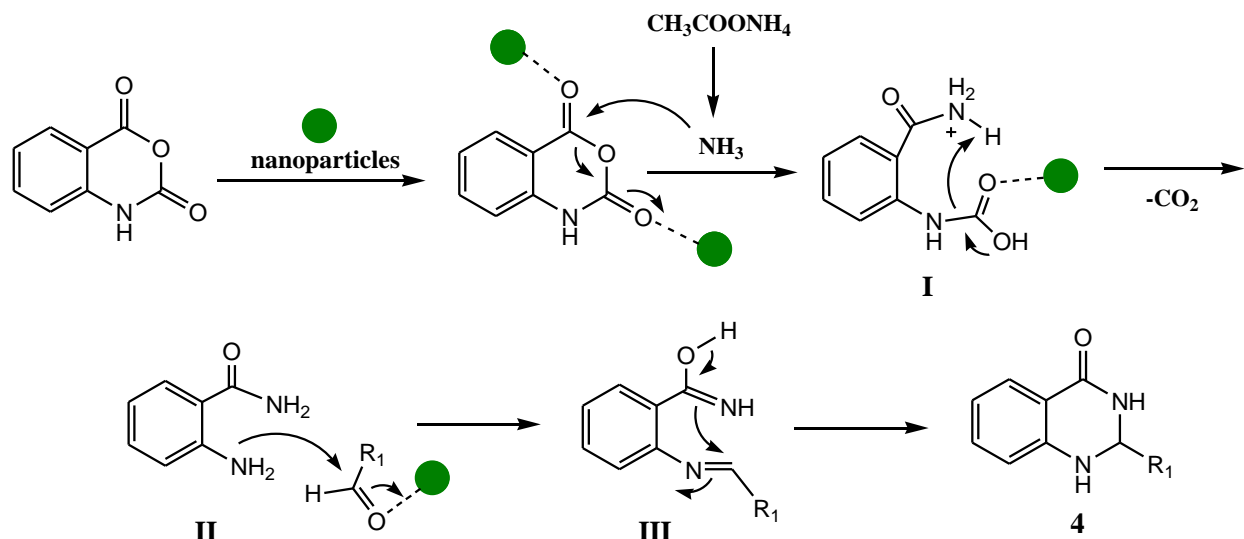
Scheme 2 Proposed mechanism for the synthesis of 2,3-Dihydroquinazolin-4(1*H*)-ones

Table 4 Synthesis of 2,3-dihydroquinazolin-4(1*H*)-one derivatives.

Number	Product	Time (min)	Yield (%)	Mp (ºC)	
				Find	Reported
9		13	95	220-222	219-221[41]
8		14	92	226-228	228-230 [42]
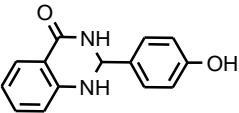
5		19	92	277-279	278-280[41]
7		16	91	204-206	206-207 [42]
6		17	90	253-255	252-254 [42]
10		11	97	194-196	197-199 [43]
11		12	95	200-201	203-205[44]
12		9	95	195-197	197-199 [43]
14		16	91	181-183	180-182 [42]
13		15	89	183-185	181-185 [42]
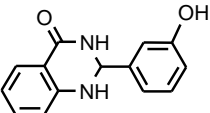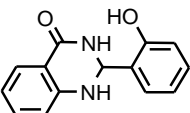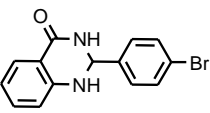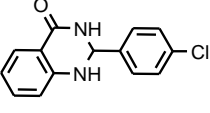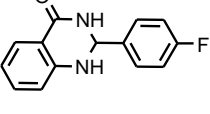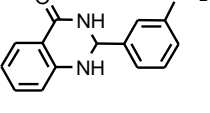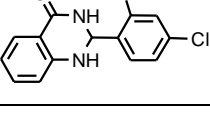
References

[1] A. Nakhaei, Z. Nakhaei, Heterocycl. Lett., 7 (2017) 565-572.

[2] E. kazemi, A. Davoodnia, A. Nakhaei, S. Basafa, N. Tavakoli-Hoseini, Adv. J. Chem. A, 1 (2018) 96-104.

[3] A. Nakhaei, A. Davoodnia, S. Yadegarian, Iran. J. Catal., 8 (2018) 47-52.

[4] J. Govan, Gun, #039, Y.K. ko, Nanomaterials, 4 (2014) 222-241.

[5] Y. Zhu, L.P. Stubbs, F. Ho, R. Liu, C.P. Ship, J.A. Maguire, N.S. Hosmane, ChemCatChem, 2 (2010) 365-374.

[6] A. Rostami, B. Tahmasbi, F. Abedi, Z. Shokri, J. Mol. Catal. A-Chem., 378 (2013) 200-205.

[7] A. Nakhaei, S. Ramezani, Iran. J. Chem. Chem. Eng., 38 (2019) 79-90.

[8] A. Nakhaei, S. Ramezani, S.J. Shams-Najafi, S. Farsinejad, Lett. Org. Chem., 15 (2018) 739-746.

[9] A. Nakhaei, S. Farsinejad, S. Ramezani, Curr. Green Chem., 4 (2017) 130-136.

[10] A. Nakhaei, A. Davoodnia, S. Yadegarian, Iran. J. Chem. Chem. Eng., 37 (2018) 33-42.

[11] A. Nakhaei, Heterocycl. Lett., 8 (2018) 579-586.

[12] M. Ghorbani, M. Aghamohammadhassan, H. Ghorbani, A. Zabihi, Microchemical Journal, 158 (2020) 105250.

[13] M. Ghorbani, M. Chamsaz, M. Aghamohammadhasan, A. Shams, Analytical biochemistry, 551 (2018) 7-18.

[14] M. Sheykhan, L. Ma'mani, A. Ebrahimi, A. Heydari, J. Mol. Catal. A-Chem., 335 (2011) 253-261.

[15] A. Nakhaei, H. Nakhaei, Heterocycl. Lett., 8 (2018) 27-33.

[16] A. Nakhaei, S. Shojaee, E. Yaghoobi, S. Ramezani, Heterocycl. Lett., 7 (2017) 323-331.

[17] G.M. Chinigo, M. Paige, S. Grindrod, E. Hamel, S. Dakshanamurthy, M. Chruszcz, W. Minor, M.L. Brown, J. Med. Chem., 51 (2008) 4620-4631.

[18] R.J. Abdel-Jalil, W. Voelter, M. Saeed, Tetrahedron Lett., 45 (2004) 3475-3476.

[19] R.C. Maia, L.L. Silva, E.F. Mazzeu, M.M. Fumian, C.M. de Rezende, A.C. Doriguetto, R.S. Corrêa, A.L.P. Miranda, E.J. Barreiro, C.A.M. Fraga, Bioorg. Med. Chem., 17 (2009) 6517-6525.

[20] R.P. Maskey, M. Shaaban, I. Grün-Wollny, H. Laatsch, J. Nat. Prod., 67 (2004) 1131-1134.

[21] J.-F. Liu, Curr. Org. Synth., 4 (2007) 223-237.

[22] M. Rueping, A.P. Antonchick, E. Sugiono, K. Grenader, Angew. Chem. Int. Ed., 48 (2009) 908-910.

[23] F. Ahmadian, A. Barmak, E. Ghaderi, M. Bavadi, H. Raanaei, K. Niknam, Journal of the Iranian Chemical Society, 16 (2019) 2647-2658.

[24] J. Chen, W. Su, H. Wu, M. Liu, C. Jin, Green Chem., 9 (2007) 972-975.

[25] A. Rostami, B. Tahmasbi, H. Gholami, H. Taymorian, Chinese Chem. Lett., 24 (2013) 211-214.

[26] K.F. Sina, A. Yahyazadeh, N.O. Mahmoodi, Letters in Organic Chemistry, 18 (2021) 176-182.

[27] P. Salehi, M. Dabiri, M.A. Zolfigol, M. Baghbanzadeh, Synlett, 2005 (2005) 1155-1157.

[28] A. Ghorbani-Choghamarani, M. Norouzi, J. Mol. Catal. A-Chem., 395 (2014) 172-179.

[29] Y.S. Kang, S. Risbud, J.F. Rabolt, P. Stroeve, Chem. Mater., 8 (1996) 2209-2211.

[30] J. Safari, Z. Zarnegar, M. Heydarian, Bull. Chem. Soc. Jpn., 85 (2012) 1332-1338.

[31] I.-T. Liu, M.-H. Hon, L.G. Teoh, Journal of electronic materials, 42 (2013) 2536-2541.

[32] Z. Gordi, M. Ghorbani, M. Ahmadian Khakhiyani, Water Environment Research, 92 (2020) 1935-1947.

[33] M. Ghorbani, S. Ariavand, M. Aghamohammadhasan, O. Seyedin, Journal of the Iranian Chemical Society, 18 (2021) 1947-1963.

[34] P. Mohammadi, M. Ghorbani, P. Mohammadi, M. Keshavarzi, A. Rastegar, M. Aghamohammadhassan, A. Saghafi, Microchemical Journal, 160 (2021) 105680.

[35] M. Ghorbani, P. Mohammadi, M. Keshavarzi, M.H. Saghi, M. Mohammadi, A. Shams, M. Aghamohammadhasan, Analytica Chimica Acta, (2021) 338802.

[36] Z. Wang, S. Zhu, S. Zhao, H. Hu, J. Alloys Compd., 509 (2011) 6893-6898.

[37] A. Barmak, K. Niknam, G. Mohebbi, ACS omega, 4 (2019) 18087-18099.

[38] M. Dabiri, P. Salehi, S. Otokesh, M. Baghbanzadeh, G. Kozehgary, A.A. Mohammadi, Tetrahedron Letters, 46 (2005) 6123-6126.

[39] M. Dabiri, P. Salehi, M. Baghbanzadeh, M.A. Zolfigol, M. Agheb, S. Heydari, Catalysis Communications, 9 (2008) 785-788.

[40] J. Safari, S. Gandomi-Ravandi, Journal of Molecular Structure, 1072 (2014) 173-178.

[41] M. Kancherla, M.R. Katlakanti, K. Seku, V. Badathala, Iran. J. Chem. Chem. Eng., 38 (2019) 37-49.

[42] S. Rostamizadeh, A.M. Amani, G.H. Mahdavinia, H. Sepehrian, S. Ebrahimi, Synthesis, 2010 (2010) 1356-1360.

[43] M. Hajjami, B. Tahmasbi, Rsc Adv., 5 (2015) 59194-59203.

[44] A. Rostami, A. Tavakoli, Chinese Chem. Lett., 22 (2011) 1317-1320.